Exploring Electron Density Evolution using Merge Tree Mappings

Florian Wetzels[1], Talha Bin Masood[2], Nanna Holmgaard List[3], Ingrid Hotz[2], Christoph Garth[1]

[1]Scientific Visualization Lab, University of Kaiserslautern-Landau, Germany [2]Scientific Visualization Group, Linköping University, Sweden
[3]Department of Chemistry, KTH Royal Institute of Technology, Sweden

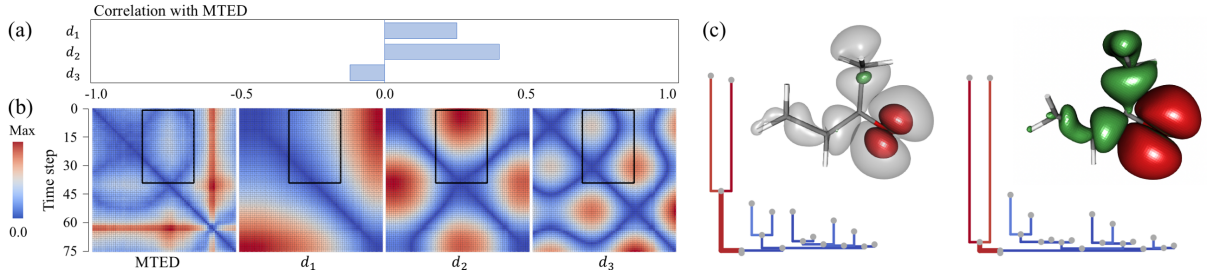

Figure 1: *The two main views of the tool prototype. On the left, four distance matrices for the time series are shown: the topological distance (MTED) for the MVK hole field and the distance of the corresponding nuclear geometries w.r.t. the three main axes of a PCA decomposition (d_1, d_2, d_3). The bar chart shows the correlation between MTED and each component for the area of interest (black box). On the right, we see two merge trees with a mapped edge highlighted. The contour rendering shows the corresponding mapped features in red.*

Abstract

This paper presents a prototypical visualization for the analysis of light-induced dynamics in molecules. It utilizes topological distances to find temporal patterns in scalar fields representing the electronic structure of such molecules and to illustrate the evolution of their features. It also provides a means to correlate these findings to the geometric evolution of the molecules.

1. Introduction

Light-driven physical and chemical processes in molecules are both critical in natural systems and underpin an ever-expanding range of technological applications ranging from photocatalysis [TLZ*17] to imaging [RCL*17] and medicine [HMT18]. The fate of the excited molecule following light absorption is dictated by the interplay between electronic changes and nuclear motion. Deciphering these intricate couplings, how they depend on the structure and their implications on charge and energy flow and hence function is an active area of research for both experiment and theory. On the theory side, *ab initio* dynamics simulations hold great promise to address these questions by providing direct access to both the evolving electronic and nuclear structures. With this comes the need to develop analysis and visualization tools that enable us to extract physical insight from the rich, time-dependent simulation data.

The output of these simulations is a time series representing the evolution of the electronic and nuclear structure. The nuclear structure is given by the relative positions of the atoms in the molecule. In this context of light-induced dynamics, we represent the electronic structure as a bivariate scalar field. On this data, we identified the following tasks to be of interest:

T1 Identifying temporal patterns in the electronic structure: are there outliers, transitions, or periodic patterns?
T2 Exploring the nature of such electronic patterns: which specific changes in the scalar field lead to these patterns?
T3 Identifying relations to changes in nuclear structure: how are electronic patterns related to changes in the molecular geometry?

Background and Related Work. Similarity measures are a basis for comparing scalar fields using clustering, outlier detection, and periodicity analysis. Recently, there has been increased interest in using topological abstractions to formulate new distance metrics for scalar fields (cf. a survey by Yan et al. [YMS*21]). For example, on the merge tree [ELZ00] (that represents the nesting of super- or sublevel sets of a scalar field) numerous distances are defined [MBW14, SMKN20, WLG22, PVDT22]. Many such distance measures for merge trees take the form of tree edit distances. These are based on structure-preserving mappings between nodes or edges of the trees. Topological abstractions like the merge tree define features of scalar fields corresponding to edges

DOI: 10.2312/evs.20241069

or nodes of the graph that can be used to derive or improve visualizations [HLH*16]. Thus, mapping-based distance measures for topological abstractions can be used to visualize correspondence of features (T2) in various settings [SSW14, WLG22, PVDT22]. They also enable more complex analysis methods based on interpolation/averaging [TMMH14, PVT23, WPTG24]. In this paper, we utilize the so-called deformation-based edit distance between merge trees [WG22] using the implementation by Wetzels et al. [WAG23].

There is rich precedent of topological methods for the analysis of electronic density fields, going back to Bader's theory of *atoms in molecules* [Bad90]. This concept has also been used for visualization purposes [GBCG*14, BGL*18, TAS*23]. For comparison of electronic charge distributions, side-by-side visualization of isosurfaces has been the norm [HG08]. A more quantitative representation is the charge transfer diagram [MTL*21], which has also been used to analyze ensembles of electronic transitions [TML*22]. A complementary perspective is provided using bivariate analysis based on continuous scatterplot operators [SMT*21].

Correlating different aspects of scientific data (T3) appears in various settings and applications. Our method is loosely related to analysis of multi-variate/multi-dimensional data [TM05, KH13, ZHQL16], or direct comparison of numerical time series [DTS*08]. As we consider a complex object per time point – the merge tree –, as opposed to numerical values, we correlate distance matrices as images. We chose a simple correlation for our prototype and reserve investigation of other area-based techniques for image registration [ZF03] (e.g. mutual information) for future work. To concisely capture the geometric motions of the molecule, we used principal component analysis (PCA) on the atom positions. Further techniques will be considered in future work [EMK*21].

Contribution. We describe a prototypical visualization design and realization, utilizing distance matrices (as heatmaps) to highlight patterns in time series of electronic structures. It provides means to explore which electronic changes over time contribute to these patterns in the topological distance. We thereby showcase that the mappings behind merge tree edit distances can indeed be used for detailed exploration of distances and changes between scalar fields. In addition, we also allow the user to inspect how these changes and patterns are connected to the nuclear structures: we determine the main modes of motion in the timeline and correlate these modes to patterns in the topological distance.

Going back to the three tasks defined above, we give a proof-of-concept for the utility of merge tree edit distances for the analysis of time-dependent electron density fields, although there are still some limitations to the approach. We showcase that interesting patterns can be found by the used distance measure and that our visualization provides means to solve all three tasks. We also discuss current limitations and how to address those in future work. An evaluation and comparison to alternative methods/distances is left for future work (see [WLG22, WAG23] for general advantages).

2. Method

We now describe the general workflow and implementation of our tool: first the input data format and preprocessing steps, which contain the majority of the computational load, then the three different

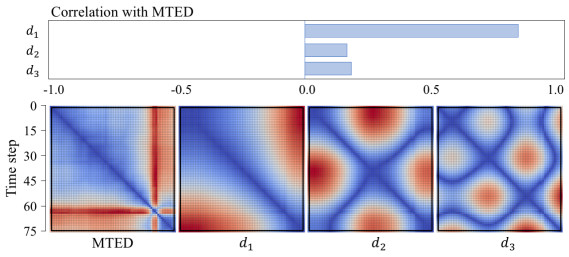

Figure 2: *The correlation and matrix views for the MVK particle field with the whole time range as area of interest.*

views of our application. Each of them visualizes a different aspect of the data and serves for a different task. All three views are active at the same time and interact. The supplementary material contains two videos showing the different views and their interaction.

2.1. Processing

Input Data. *Ab initio* dynamics simulations output a time series representing nuclear and electronic structure per time step. Each nuclear structure is given as a point cloud $P = \{p_1, \cdots, p_n\}$, where n is the number of atoms and p_i is the spatial location of atom i. Visual representations of chemical bonding are computed based on a geometric heuristic [SHYL23] to yield a 3D-embedded graph. We represent the excited electronic structure in terms of a natural transition orbitals (NTO) decomposition [Mar03], providing a compact representation of the one-electron transition density in terms of hole and particle orbital pairs (labeled $\phi_h, \phi_p : \mathbb{R}^3 \to \mathbb{R}$) that indicate the electronic movement upon excitation.

Density Field Computation and Simplification. For each time step, a structured grid representation of the absolute hole and particle fields, $|\phi_h(t)|$ and $|\phi_p(t)|$, is computed from the NTO representation of the orbitals. We analyze the topology of the electron structure for hole and particle separately. Motivated by practical

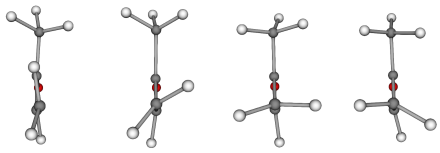

(a) *The rotation at time steps 0, 45, 61 and 74 (left to right).*

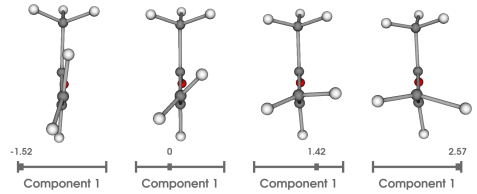

(b) *The rotation for different values of the first component.*

Figure 3: *The rotation of the two hydrogen atoms shows up in the time series as well as the first component of the PCA.*

considerations, we use absolute values, as then all relevant topological features are maxima of the scalar field, enabling the use of merge trees instead of contour trees for analysis. Per density field in the time series, we perform topological simplification using a persistence threshold of 1% of the scalar range.

Merge Tree Computation and Layout. For each simplified density field, we compute its augmented join tree (since we are interested in *maxima* of the *absolute* density). To draw the merge trees in a 2D view, we compute a planar layout for each merge tree. The simplified scalar fields, the segmentations, the merge trees and their layouts are all computed once in a preprocessing procedure using TTK [TFL*18] and then stored on disk.

Distance Matrix Computation. We compute a distance matrix based on the so-called *deformation-based edit distance* [WG22] (from now on refered to as MTED) for the hole and particle time series using an adaptation of the implementation provided in [WAG23]. The implementation finds an optimal mapping and its cost through an integer programming encoding the structural constraints of an edit distance. Thus, further constraints can be added in a straight-forward manner. We restricted the allowed mappings by geometric constraints: for each leaf node in the merge tree, we compute its closest atom through a Voronoi tesselation of the domain. Then, we only allow two leaves to be mapped, if their closest atom matches. We also propagate the leaf constraints to inner nodes of the tree. The distance matrix and all mappings (for each pair of trees) are computed once in a preprocessing step and stored as dictionary objects. The distance computations constitute the main computational load of the whole workflow, since the distance used has been shown to be NP-complete [WAG23]. However, we were able to compute the full distance matrix on the MVK dataset (Secion 3) in around 20 minutes using the application-specific constraints described above. They also enabled feasible running times on merge trees of up to 60 nodes. For even larger data, we should note that all methods presented also can be applied using more efficient (but also less expressive) edit distances such as those presented in [SMKN20, PVDT22, WLG22, WG22].

Principal Component Analysis. In addition to the MTED matrix, we also compute three more distance matrices based on the nuclear structures. In contrast to the MTEDs, they are computed on startup. Each atom position in a molecule is a 3D point. For a molecule $\{p_1, \cdots, p_n\}$, we can thus create a $3n$-dimensional vector encoding all atom positions by simply concatenating all 3D points. When creating this encoding for each molecule, we get a $3n$-dimensional point cloud. On this point cloud, we perform a principal component analysis and extract the three main axes (we refer to them as c_1, c_2, c_3). Each molecule then corresponds to a point in this three-dimensional space. For two molecules with positions $m_1 = (c_1^1, c_2^1, c_3^1)$ and $m_2 = (c_1^2, c_2^2, c_3^2)$ in the PCA target space, we now define the distance $d_1(m_1, m_2) = |c_1^1 - c_1^2|$ and d_2, d_3 analogous. We then compute three distance matrices based on d_1, d_2, d_3.

2.2. Visualization

Matrix and Correlation View. The main window of our application is the matrix and correlation view (Figure 2). It shows the four distance matrices based on the MTED, d_1, d_2 and d_3 in this order. Furthermore, it allows to overlay a submatrix selection (the black box), which can be defined by the user. For this subset of distances, we compute the correlation between the values of MTED and each of d_1, d_2, d_3. The correlation view shows these three correlation values as a bar chart, see correlation panel in Figures 1 or 2. It also contains general settings such as which scalar field should be considered ($|\phi_h(t)|$ or $|\phi_p(t)|$).

PCA and Timeline View. To explain the physical meaning the aforementioned components of motion, we provide the PCA and timeline view. It shows the nuclear structure as a 3D-embedded graph together with three sliders, one for each component. Their values represent a point in the 3D target space of the PCA. It is projected back to molecule geometry and rendered. The window also has an alternative mode to investigate the original time series of nuclear structures using a single slider (cf. supplementary video).

Merge Tree View. The merge tree view visualizes feature evolutions/changes for two specific time steps. It directly interacts with the matrix view: the user can click into the distance matrix to select a pair of time steps which needs further analysis. The merge tree view then renders the two merge trees and the two 3D scalar fields through isosurfaces (see Figure 1(c)). The molecule geometries are embedded in the scalar field rendering to provide further context. The user can either modify the rendered isovalue manually or choose it through interaction with the merge tree drawing.

The edges of the two merge trees are colored such that they show where changes happen in terms of MTED. In an edit mapping, each edge of a tree is either mapped to an edge in the other tree or deleted. The cost of this operation (relative to the total distance between the two trees) is shown through the edge colors. Thus, red edges show that the corresponding feature changes/evolves substantially between the two time steps, whereas blue edges stay more consistent. When the user clicks an edge, the isovalue of the corresponding scalar field is set to the center of its scalar range and the corresponding feature is colored in red. The edge itself is highlighted through stroke width. If the selected edge is mapped the same happens for the second tree. Thus, the tree view shows which edges are mapped as well as which scalar field features are mapped. Note that both renderings show different isovalues. To accommodate this, the second isovalue is shown using transparent gray isosurfaces (cf. Figure 4a). If the selected edge is deleted, the second view will not show any isosurfaces except the transparent one encoding the selected value of the other view (cf. Figure 4b).

3. Results

We now apply our method to a dataset representing light-induced dynamics of methylvinylketone [CCL23] (MVK, Figure 1(c)), a molecule present in the lower atmosphere. We consider the excited S_1 state by following the evolution of its hole and particle orbitals separately. We obtain 75 time steps and merge trees with around 30 vertices. The molecular skeleton is planar in the ground state, but upon light absorption, it rotates the terminal C=C double bond, bringing the two vinyl hydrogen (rendered white) atoms out of the plane. Figure 3a shows four time steps in different stages of the rotation.Upon reaching a perpendicular conformation (steps 61-63),

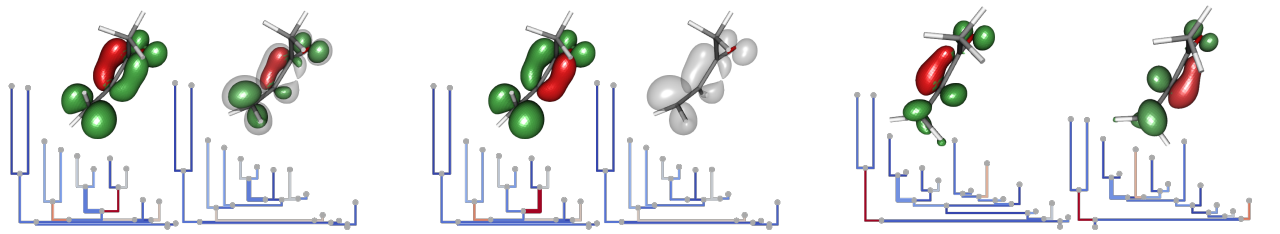

(a) *Time step 3 vs 47: mapped structure* **(b)** *Time step 3 vs 47: deleted structure* **(c)** *Time step 59 vs 70: mapping of mirrored structure*

Figure 4: *Feature changes in the MVK particle field between different stages of the rotation, as seen in the merge tree view: the region corresponding to the selected edge (thicker stroke) is highlighted as a red contour. For unmapped edges, the second view is empty, see (b).*

we expect substantial changes in the electronic structure due to electronic state crossings between the S_2 and S_1 states [CCL23]. After performing PCA, the first component captures the described rotation, see Figure 3b. The corresponding matrix reveals that the nuclear structure changes consistently along this axis (Figure 2, d_1).

We now consider the MTED matrix for the particle field (Figure 2, MTED). Overall, it shows a similar evolution over time as d_1, which is also highlighted by a high overall correlation between them (see Figure 2, correlation panel). The only major difference are the three outlier time steps in the MTED matrix at time steps 61-63. As stated above, abrupt changes in the electronic structure are expected for exactly these time steps. Thus, we can conclude that the MTED highlights the electronic state crossing (T1), while otherwise capturing the changes along the main motion (T3).

To understand how the MTED on the particle field caputures the rotational motion, we consider symmetry of both nuclear and electronic structure. In the beginning of the rotation, the nuclear geometry is planar and the distribution of electron density is symmetric around this plane (see left rendering in Figure 4a). However, when the two vinyl hydrogen atoms rotate out of plane, the electronic symmetry is broken accordingly (T2). While on one side there is a feature merging the two maxima at the center carbon (rendered gray) atoms, there is no such feature on the other side (see right rendering in Figure 4a). Thus, when comparing to an early time step in the merge tree view, only one such feature can be matched (Figure 4a), but has to be deleted on the other side (Figure 4b). When the two hydrogen atoms become perpendicular to the plane, we obtain the outlier behavior discussed above with a symmetric electronic structure, though different from the earlier one. In the time steps after the outliers, we get the asymmetric electronic structure again, however, the density maxima are flipped on the symmetry plane, see Figure 4c (T2). This also shows in the blue areas around the outlier stripe in the MTED matrix in Figure 2 (T1).

The MTED matrix for the hole field shows more complex patterns than the one for the particle field. A prominent feature is the wing-shaped structure in the first half of the time series (T1), see boxed area in Figure 1(b). When exploring the feature changes of this pattern, we can see that it is caused by a shift of the saddle connecting the two maxima around the oxygen (rendered red) atom (T2), see Figure 1(c). Discussions with a domain scientist revealed that this saddle movement is actually a resolution artifact, but still has meaning as it is probably caused by a change in gradient. Furthermore, we found that correlation with nuclear motions (T3) is limited (no clear correlation visible). This is probably due to the linear nature of PCA, whereas certain vibrational modes are inherently curvilinear, such as torsional degrees of freedom. For example, when increasing c_1 further than the vertical alignment, one of the rotated hydrogen atoms seems to "fly away" (Figure 3b), indicating a poor linear approximation.

The supplementary material contains a video showing that our method is also feasible on larger datasets (200 time steps, 50-70 merge tree nodes). It shows that the MTED is able to correctly identify a bond formation within the time series. However, we believe a detailed discussion to be beyond the scope of a short paper.

4. Conclusion and Future Work

We showed that the matrix view highlights temporal patterns, e.g. outliers, in electron density time series (T1). The found outliers indeed correspond to established relevant time steps of interest. The merge tree view is able to reveal the nature of these patterns (T2), e.g. saddle shift or electronic symmetry. Discussions with a domain scientist exposed that some feature changes are rooted in artifacts induced by discretization, which shows that such an analysis is important and necessary. Some patterns could be correlated with nuclear motion found through PCA (T3). However, in this task lie the most important limitations of our current approach: we need to incorporate non-linear decomposition methods, as physical motions are often non-linear. Furthermore, simple correlation as a means to find relation between nuclear and electronic evolution could also be replaced through other techniques, e.g. from the field of image registration. Other possibilities for future work include improved interaction with the feature mappings (currently it requires solid understanding of the merge tree concept) or integrating the sign of the electron density, both visually and as additional constraints on the considered mappings/distance. In addition, as this paper only provided proof-of-concept, a proper design study should be conducted to formally evaluate the chosen method against alternatives.

Acknowledgments This research was supported by the German Research Foundation (DFG): 442077441; the Swedish e-Science Research Center (SeRC); the Swedish Research Council (VR): 2019-05487, 2022-02871, 2023-04806; and, Wallenberg Autonomous Systems and Software Program (WASP) funded by the Knut and Alice Wallenberg Foundation. The simulations were enabled by the super-computing resource Berzelius provided by the National Supercomputer Centre (NSC) at Linköping University and the Knut and Alice Wallenberg Foundation.

References

[Bad90] BADER R. F. W.: *Atoms in molecules – A Quantum Theory*. International Series of Monographs on Chemistry. Wiley Online Library, 1990. 2

[BGL*18] BHATIA H., GYULASSY A. G., LORDI V., PASK J. E., PASCUCCI V., BREMER P.-T.: TopoMS: Comprehensive topological exploration for molecular and condensed-matter systems. *J. Comp. Chem. 39*, 16 (2018), 936–952. 2

[CCL23] CHAKRABORTY P., COUTO R. C., LIST N. H.: Deciphering methylation effects on s2(ππ*) internal conversion in the simplest linear α,β-unsaturated carbonyl. *J. Phys. Chem. A 127*, 25 (2023), 5360–5373. PMID: 37331016. 3, 4

[DTS*08] DING H., TRAJCEVSKI G., SCHEUERMANN P., WANG X., KEOGH E. J.: Querying and mining of time series data: experimental comparison of representations and distance measures. *Proc. VLDB Endow. 1*, 2 (2008), 1542–1552. 2

[ELZ00] EDELSBRUNNER H., LETSCHER D., ZOMORODIAN A.: Topological persistence and simplification. In *41st Ann. Symp. on Foundations of Computer Science, FOCS 2000, 12-14 November 2000, Redondo Beach, California, USA* (2000), IEEE Computer Society, pp. 454–463. 1

[EMK*21] ESPADOTO M., MARTINS R. M., KERREN A., HIRATA N. S. T., TELEA A. C.: Toward a quantitative survey of dimension reduction techniques. *IEEE Transactions on Visualization and Computer Graphics 27*, 3 (2021), 2153–2173. 2

[GBCG*14] GÜNTHER D., BOTO R. A., CONTRERAS-GARCÍA J., PIQUEMAL J.-P., TIERNY J.: Characterizing molecular interactions in chemical systems. *IEEE Transactions on Visualization and Computer Graphics (TVCG) 20*, 12 (2014), 2476–2485. 2

[HG08] HARANCZYK M., GUTOWSKI M.: Visualization of molecular orbitals and the related electron densities. *Journal of Chemical Theory and Computation 4*, 5 (2008), 689–693. 2

[HLH*16] HEINE C., LEITTE H., HLAWITSCHKA M., IURICICH F., FLORIANI L. D., SCHEUERMANN G., HAGEN H., GARTH C.: A survey of topology-based methods in visualization. *Comput. Graph. Forum 35*, 3 (2016), 643–667. 2

[HMT18] HULL K., MORSTEIN J., TRAUNER D.: In vivo photopharmacology. *Chemical reviews 118*, 21 (2018), 10710–10747. 1

[KH13] KEHRER J., HAUSER H.: Visualization and visual analysis of multifaceted scientific data: A survey. *IEEE Transactions on Visualization and Computer Graphics 19*, 3 (2013), 495–513. 2

[Mar03] MARTIN R. L.: Natural transition orbitals. *The Journal of Chemical Physics 118*, 11 (2003), 4775–4777. 2

[MBW14] MOROZOV D., BEKETAYEV K., WEBER G. H.: Interleaving distance between merge trees. In *TopoInVis*. 2014. 1

[MTL*21] MASOOD T. B., THYGESEN S. S., LINARES M., ABRIKOSSOV A., NATARAJAN V., HOTZ I.: Visual analysis of electronic densities and transitions in molecules. *Computer Graphics Forum 40*, 3 (2021). 2

[PVDT22] PONT M., VIDAL J., DELON J., TIERNY J.: Wasserstein distances, geodesics and barycenters of merge trees. *IEEE Trans. Vis. Comput. Graph. 28*, 1 (2022), 291–301. 1, 2, 3

[PVT23] PONT M., VIDAL J., TIERNY J.: Principal geodesic analysis of merge trees (and persistence diagrams). *IEEE Trans. Vis. Comput. Graph. 29*, 2 (2023), 1573–1589. 2

[RCL*17] RODRIGUEZ E. A., CAMPBELL R. E., LIN J. Y., LIN M. Z., MIYAWAKI A., PALMER A. E., SHU X., ZHANG J., TSIEN R. Y.: The growing and glowing toolbox of fluorescent and photoactive proteins. *Trends in Biochemical Sciences 42*, 2 (2017), 111–129. 1

[SHYL23] SKÅNBERG R., HOTZ I., YNNERMAN A., LINARES M.: Viamd: a software for visual interactive analysis of molecular dynamics. *J. Chem. Inf. Model 63*, 23 (2023), 7382. 2

[SMKN20] SRIDHARAMURTHY R., MASOOD T. B., KAMAKSHIDASAN A., NATARAJAN V.: Edit distance between merge trees. *IEEE Trans. Vis. Comput. Graph. 26*, 3 (2020), 1518–1531. 1, 3

[SMT*21] SHARMA M., MASOOD T. B., THYGESEN S. S., LINARES M., HOTZ I., NATARAJAN V.: Segmentation driven peeling for visual analysis of electronic transitions. In *IEEE VIS Short Papers* (2021). 2

[SSW14] SAIKIA H., SEIDEL H., WEINKAUF T.: Extended branch decomposition graphs: Structural comparison of scalar data. *Comput. Graph. Forum 33*, 3 (2014), 41–50. 2

[TAS*23] THYGESEN S. S., ABRIKOSOV A. I., STENETEG P., MASOOD T. B., HOTZ I.: Level of detail visual analysis of structures in solid-state materials. In *EuroVis Short Papers* (2023). 2

[TFL*18] TIERNY J., FAVELIER G., LEVINE J. A., GUEUNET C., MICHAUX M.: The topology toolkit. *IEEE Trans. Vis. Comput. Graph. 24*, 1 (2018), 832–842. 3

[TLZ*17] TWILTON J., LE C., ZHANG P., SHAW M. H., EVANS R. W., MACMILLAN D. W.: The merger of transition metal and photocatalysis. *Nature Reviews Chemistry 1*, 7 (2017), 0052. 1

[TM05] TEOH S. T., MA K.: Hifocon: Object and dimensional coherence and correlation in multidimensional visualization. In *Proc. 1st Int. Symp. on Advances in Visual Computing ISVC, 2005, Lake Tahoe, NV, USA* (2005), vol. 3804 of *Lecture Notes in Computer Science*, Springer, pp. 235–242. 2

[TML*22] THYGESEN S. S., MASOOD T. B., LINARES M., NATARAJAN V., HOTZ I.: Level of detail exploration of transition diagram ensembles. *Computer Graphics Forum 41*, 3 (2022). 2

[TMMH14] TURNER K., MILEYKO Y., MUKHERJEE S., HARER J.: Fréchet means for distributions of persistence diagrams. *Discret. Comput. Geom. 52*, 1 (2014), 44–70. 2

[WAG23] WETZELS F., ANDERS M., GARTH C.: Taming horizontal instability in merge trees: On the computation of a comprehensive deformation-based edit distance. In *2023 Topological Data Analysis and Visualization (TopoInVis)* (2023), pp. 82–92. 2, 3

[WG22] WETZELS F., GARTH C.: A deformation-based edit distance for merge trees. In *2022 Topological Data Analysis and Visualization (TopoInVis)* (2022), pp. 29–38. 2, 3

[WLG22] WETZELS F., LEITTE H., GARTH C.: Branch decomposition-independent edit distances for merge trees. *Comput. Graph. Forum 41*, 3 (2022), 367–378. 1, 2, 3

[WPTG24] WETZELS F., PONT M., TIERNY J., GARTH C.: Merge tree geodesics and barycenters with path mappings. *IEEE Trans. Vis. Comput. Graph. 30*, 1 (2024), 1095–1105. 2

[YMS*21] YAN L., MASOOD T. B., SRIDHARAMURTHY R., RASHEED F., NATARAJAN V., HOTZ I., WANG B.: Scalar field comparison with topological descriptors: Properties and applications for scientific visualization. *Comput. Graph. Forum 40*, 3 (2021), 599–633. 1

[ZF03] ZITOVÁ B., FLUSSER J.: Image registration methods: a survey. *Image Vis. Comput. 21*, 11 (2003), 977–1000. 2

[ZHQL16] ZHANG H., HOU Y., QU D., LIU Q.: Correlation visualization of time-varying patterns for multi-variable data. *IEEE Access 4* (2016), 4669–4677. 2